

# Deep Reinforcement Learning for Electric Vehicle Routing Problem with Time Windows

Bo Lin, Bissan Ghaddar, Jatin Nathwani,

**Abstract**—The past decade has seen a rapid penetration of electric vehicles (EV) in the market, more and more logistics and transportation companies start to deploy EVs for service provision. In order to model the operations of a commercial EV fleet, we utilize the EV routing problem with time windows (EVRPTW). In this research, we propose an end-to-end deep reinforcement learning framework to solve the EVRPTW. In particular, we develop an attention model incorporating the pointer network and a graph embedding technique to parameterize a stochastic policy for solving the EVRPTW. The model is then trained using policy gradient with rollout baseline. Our numerical studies show that the proposed model is able to efficiently solve EVRPTW instances of large sizes that are not solvable with any existing approaches.

**Index Terms**—Deep reinforcement learning, electric vehicle routing problem with time windows

## I. INTRODUCTION

ELECTRIC vehicles (EV) has been playing an increasingly important role in urban transportation and logistics system for their capabilities of reducing greenhouse gas emission, promoting renewable energy etc. [1], [2]. To model the operations of logistic companies using EVs for service provision, Schneider et al. proposed the electric vehicle routing problem with time windows (EVRPTW) [3]. In the context of EVRPTW, a fleet of capacitated EVs are responsible for serving customers located in a specific region; each customer is associated with a demand that must be satisfied during a time window; all the EVs are fully charged at the start of the planning horizon and could visit charging stations anytime to fully charge their batteries. The objective is to find routes for the EVs such that total distance travelled by the fleet is minimized.

As an NP-hard optimization problem (CO), solving the EVRPTW is computationally expensive. Schneider et al. [3] developed a variable neighborhood search and tabu search hybrid meta-heuristic (VNS/TS) that is able to effectively solve benchmark instances. In a later paper [4], Desaulniers et al. proposed exact branch-and-price-and-cut algorithms for four variants of the EVRPTW according to the number of recharges and the type of recharges. Both algorithms are able to provide high-quality solutions to the EVRPTW benchmark instances with 100 customers and 21 stations, yet the solution quality

and efficiency decrease as instance size increases. In addition, both algorithms have components that require extensive hand-engineering, making it difficult to generalize these algorithms to other EVRPTW variants.

This research is motivated by an emerging group of literature on utilizing advanced deep learning techniques to solve CO. There are two typical paradigms: supervised learning and reinforcement learning (RL). Supervised learning models, as the ones presented in [5], [6], [7] and [8], are trained with solutions provided by existing algorithms. Although they could generate near-optimal solutions to the problems they are trained on [5] and could generalize to instances from different distributions [7] and of larger sizes than the ones they have seen during training [6], supervised approaches are not applicable to most CO problems because one does not have access to optimal labels [9].

On the other hand, RL models, such as the ones presented in [10], [11], [12], [9], [13], [14] and [15], could learn to tackle CO even without optimal labels. They consider solving problems through taking a sequence of actions similar to Markov decision process (MDP). Some reward schemes are designed to inform the model about the quality of the actions it made based on which model parameters are adjusted to enhance solution quality. It has already been successfully applied to various COs such as the travelling salesman problem (TSP), vehicle routing problem (VRP), minimum vertex cover (MVC), maximum cut (MAXCUT) etc. Despite the difficulty in training deep RL models, it is currently accepted as a very promising research direction to pursue.

The main objective of this research is to develop a RL model to solve EVRPTW. In particular, based on the framework proposed by Nazari et al. [14] for VRP and TSP, we re-define the system state, rewarding schemes as well as the masking policy for EVRPTW. The original framework in [14] only considers representation of vertex information and does not take into account graph structure as well as global information which is very important in EVRPTW. To this end, we incorporate the model with a graph embedding component put forward by Dai et al. [16] to synthesize local and global information of the graph on which the problem is defined. The model is then trained using the REINFORCE gradient estimator with greedy rollout baseline [15].

The proposed model is able to efficiently generate good feasible solutions to EVRPTW instances of very large sizes that are unsolvable with any existing methods. It, therefore, could be implemented to support large-scale real-time EV fleet operations. Moreover, the solutions generated by the RL model could be fed to other solution algorithms as starting points or search tree trimmer, which could possibly assist

B. Lin is with the Department of Mechanical and Industrial Engineering, University of Toronto, Toronto, ON M5S 3G8 Canada (email: blin@mie.utoronto.ca). This work was done during his master's at the University of Waterloo.

B. Ghaddar is with Ivey Business School, Western University, London, ON N6G 0N1 Canada (email: bghaddar@ivey.uwo.ca).

J. Nathwani is with the Department of Management Sciences, University of Waterloo, Waterloo, ON N2L 3G1 Canada (email: b46lin@uwaterloo.ca; nathwani@uwaterloo.ca).

to enhance solution efficiency. Furthermore, the model has potential to generalize to other variants of EVRPTW through slightly tailoring the rewarding scheme and masking policy.

The remainder of the paper is structured as follows. We review previous related literature in Section II, and formally introduce the problem formulation in Section III. We then describe the reinforcement learning framework for EVRPTW in Section IV and provide detailed illustration on our methodology in Section V. Computational results and analysis about the proposed approach are presented in Section VI. Finally, we conclude the paper and suggest some possible extensions of the proposed method in Section VII.

## II. RELATED WORK

The application of neural network (NN) to solving CO dates back to the paper by Hopfield and Tank [17]. They define an array representation for TSP solutions. In an  $n$ -city TSP instance, each city  $I$  is associated with an  $n$ -dimensional array  $V_I$  whose  $i^{th}$  entry  $v_{I,i}$  takes a value of 1 if city  $I$  is the  $i^{th}$  city along the route and takes 0 otherwise. All the city arrays form an  $n \times n$  array modeled by  $n^2$  neurons. Some motion equations were constructed to describe the time evolution of the circuit in the analogy network comprised of the neurons. The circuit finally converge to a "low-energy" state favoring high quality feasible solutions to the TSP. Although a later paper by Wilson and Pawley [18] points out that the NN proposed in [17] does not have a learning process, and its performance heavily relies on the choice of model parameters which compromises its scalability and the generalization capability, it stimulated various related research on applying NN to solve CO.

One promising direction is to solve CO by learning a value function to evaluate each possible adjustment in the current solution or action for constructing solutions. The value function can then be utilized by search algorithms to find good solutions to the target problem. For example, for a job-scheduling problem of NASA, Zhang et al. [10] parameterize such a value function as an NN that intakes some hand-designed features of the current schedule and outputs the "value" of the possible adjustments. For CO that is defined on a graph, hand designed features could be replaced by graph embedding networks that synthesize the structure as well as local and global information of the graph. Khalil et al. [13] use fitted-Q learning to train a graph embedding network (DQN) for action evaluation based on which they greedily decode solutions to target problems including TSP, MVC and MAXCUT. Other graph embedding examples could be seen in [6], [7] and [8], though the embedded graph vectors in [7] and [8] are fed to NN to predict problem-specific values instead of evaluating actions.

While [10] and [13] mainly focus on how to construct NN to estimate values of actions, there are some other research concentrating on the decoding process based on the value function. For the maximum independent set problem, Li et al. [6] argue that the naive decoding method, i.e. to greedily select the vertex with the highest value, might lead to poor results because there might exist many optimal solutions and each vertex could participate in some of them. To address the

issue, they propose a tree search paradigm supported by the value function enabling the algorithm to explore a diverse set of solutions. A graph reduction and a local search component were incorporated to enhance solution efficiency and quality. To further accelerate the searching process, Mittal et al. [11] propose a graph convolution network to prune poor vertices and learn the embeddings of good vertices which are then fed to the model of Li et al. [6] to produce solution set. Moreover, Barrett et al. [12] proposed the exploratory DQN allowing the algorithm to revise the actions it previously made so as to more comprehensively explore the solution space.

There is another group of research on applying policy-based approaches, which learn policies to directly determine the next action given a system state, to solve CO. One good example is the pointer network (PN) developed by Vinyals et al. [5] for CO, such as TSP and VRP, whose solutions are permutations of the given vertices. Inspired by the sequence-to-sequence learning [19] originally proposed for machine translation, the PN intakes the given vertices and predict a permutation of them. The PN is trained in a supervised manner with instance-solution pairs generated by an approximate solver. To generalize the PN to CO for which instance-solution pairs are difficult to obtain, Bello et al. [9] used a policy gradient method to train the PN. The PN is able to efficiently find close-to-optimal solutions to TSP instances with up to 100 vertices. Nazari et al. [14] further generalized this method to the VRP whose vertex states change during the decoding process. Considering that the order of the vertices does not provide any additional information for a VRP solver, they replace the RNN encoder in the PN with element-wise projections of vertex information which accelerates the model implementation. On the other hand, Kool et al. [15] propose a multi-head attention model for the TSP and VRP. The model is trained using policy gradient with roll-out baseline which is easier to implement in practice than the A3C method utilized by [14].

Although value-based methods perform well on various CO problems, they do not directly apply to EVRPTW since some vertices (stations and the depot) could appear more than once in a solution. Given the similarity between the VRP and the EVRPTW, the policy-based framework proposed by Nazari et al. [14] is a better fit to the EVRPTW, yet global information of the system, which is very important for solving EVRPTW, should also be taken into consideration. Hence, our proposed model is based on the framework of [14] and incorporates a graph embedding component proposed by [13] to synthesize the local and global information of the network.

With a very similar idea, Yu et al. [20] incorporate the Structure2Vec tool [16] with PN [5] to develop a distributed system for solving an online routing problem. Zhao et al. [21] extend the work of [14] to VRPTW by revising the masking scheme and adding a local search phase to further improve the solution provided by the attention model. Our proposed approach differs from them in terms of model architecture, training method as well as problem settings.

## III. EVRPTW

The EVRPTW proposed by [3] is illustrated in Figure 1. We are given a set of customers scattered in a region, each is

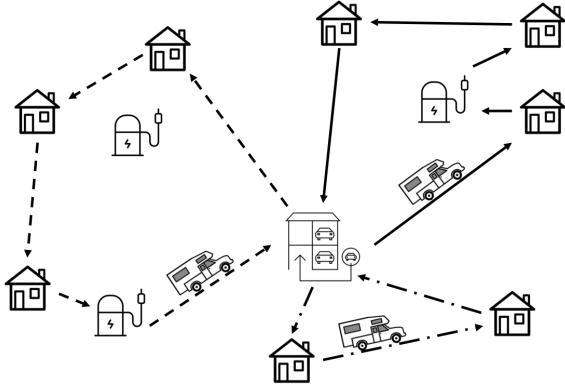


Fig. 1. The electric vehicle routing problem with time windows

associated with a demand that need to be satisfied by an EV during a time window. A fleet of capacitated EVs are initially placed at a depot and are fully charged. They could leave the depot to serve the customers and visit stations to recharge their batteries during the planning horizon. Every time an EV visits a charging station, its battery will be fully charged using linear charging time. By the end of the planning horizon, they are supposed to return to the depot. We seek to find routes for the EVs such that all the customer demands are satisfied during their time windows and the total distance travelled by the fleet is minimized.

In order to fit the framework of [14], we define the EVRPTW on a graph where there are 3 types of vertices: customer ( $V_c$ ), station ( $V_s$ ) and depot ( $V_d$ ). Each vertex  $i$  is associated with an array  $X_i^t = (x_i, z_i, e_i, l_i, d_i^t)$  where  $x_i$  and  $z_i$  represent the geographical coordinate of vertex  $i$ ,  $e_i$  and  $l_i$  represent the corresponding time window, and  $d_i^t$  is the remaining demand at vertex  $i$  at decoding step  $t$ . We superscript  $d_i$  and  $X_i$  with step  $t$  because we solve the problem in a sequential manner, which will be elucidated in Section IV, and these two elements could change over time. All the other elements in  $X_i^t$  are static. We do not consider the service time at each vertex as [3] because we assume it to be a constant to simplify the problem. All the vertex arrays form a set  $X^t$  that describes the local information at the vertices at decoding step  $t$ . The graph is complete, the weight of each edge is the euclidean distance between the connected vertices.

Besides, these nodes share a set of global variables  $G^t = \{\tau^t, b^t, ev^t\}$  where  $\tau^t$ ,  $b^t$  and  $ev^t$  indicate the time, battery level of the active EV and the number of EV(s) available at the start of decoding step  $t$  respectively. The values of  $\tau^t$  and  $ev^t$  are initially set to 0 and the size of the fleet respectively. The value of  $b^t$  is initialized as an EV's battery capacity. All the global variables could change over time. We note that, we do not list EV cargo as a global variable here because it is not an input to the model that is introduced in Section V. But we do keep track on the EV's remaining cargo for the masking scheme implementation.

A solution to the EVRPTW is a sequence of vertices in the graph that could be interpreted as the EVs' routes. Routes for different EVs are separated by the depot. For instance, suppose vertex 0 represents the depot, vertex sequence

$\{0, 3, 2, 0, 4, 1, 0\}$  corresponds to two routes: one travels along  $0 \rightarrow 3 \rightarrow 2 \rightarrow 0$ , the other one travels along  $0 \rightarrow 4 \rightarrow 1 \rightarrow 0$ .

#### IV. REINFORCEMENT LEARNING FOR EVRPTW

In this section, we describe the problem in a reinforcement learning fashion. We assume that there is an agent who seeks to generate a solution to the EVRPTW by taking a sequence of actions. In particular, at each step, the agent intakes the current system state and makes an action based on the given information. The system state then changes as a consequence. This procedure is repeated until certain termination conditions are met. We train the agent with numerous EVRPTW instances and use a reward function to evaluate the solutions generated by the agent and guide the agent to improve accordingly.

In the context of EVRPTW, the system state is the representation of the graph information  $X^t$  and  $G^t$ . An action is to add (decode) a vertex to the end of the current sequence. We use  $y^t$  to denote the vertex we select at step  $t$  and  $Y^t$  to denote the vertex sequence we form up to step  $t$ . The termination condition is that all the customer demands are satisfied. We assume the procedure is terminated at step  $t_m$ .

More specifically, at each decoding step  $t$ , given  $G^t$ ,  $X^t$  and travel history  $Y^t$ , we estimate the probability of adding each vertex  $i$  to the sequence  $P(y^{t+1} = i | X^t, G^t, Y^t)$ , and decode the next vertex to visit  $y^{t+1}$  according to this probability distribution. Based on  $y^{t+1}$ , we update the system states using transition functions (1) - (4).

First, system time  $\tau^{t+1}$  is updated as follows.

$$\tau^{t+1} = \begin{cases} \max(\tau^t, e_{y^t}) + s + t(y^t, y^{t+1}), & \text{if } y^t \in V_c \\ \tau^t + t(y^t, y_{t+1}) + re(b^t), & \text{if } y^t \in V_s \\ t(y^t, y^{t+1}), & \text{otherwise} \end{cases} \quad (1)$$

where  $t(y^t, y^{t+1})$  is the travelling time from vertex  $y^t$  to vertex  $y^{t+1}$ ,  $re(b^t)$  is the time required to fully charge the battery from the given level  $b^t$ ,  $s$  is a constant representing the service time at each customer vertex.

Next, the battery level of the active EV is updated:

$$b^{t+1} = \begin{cases} b^t - f(y^t, y^{t+1}), & \text{if } y^t \in V_c \\ B - f(y^t, y^{t+1}), & \text{otherwise} \end{cases} \quad (2)$$

where  $f(y^t, y^{t+1})$  is the energy consumption of the EV travelling from vertex  $y^t$  to vertex  $y^{t+1}$ ,  $B$  is the battery capacity.

Finally, the number of EVs available  $ev^t$  and the remaining demands at each vertex  $d_i^t$  are updated as follows.

$$ev^{t+1} = \begin{cases} ev^t - 1, & \text{if } y^t \in V_d \\ ev^t, & \text{otherwise} \end{cases} \quad (3)$$

$$d_i^{t+1} = \begin{cases} 0, & y^t = i \\ d_i^t, & \text{otherwise} \end{cases} \quad (4)$$

We define the reward function for a vertex sequence  $Y^{t_m} = \{y^0, y^1, \dots, y^{t_m}\}$  as in Equation (5). A high reward value corresponds to a solution of high quality. Given that the objective of the EVRPTW is to minimize the total distance

traveled by the fleet, we set the first term in Equation (5) as the negative total distance travelled by the fleet in favor for short-distance solutions. The other terms are penalties of problem constraint violations. If a solution  $Y^{t_m}$  requires more than the given EVs, the corresponding  $ev^{t_m}$  will be negative which is penalize in the second term. Moreover, if the depot is located very close to a station, we observe through experiments that the model might achieve low travelling distance by constantly moving between this station and the depot without serving any customers. In order to prevent this issue, we introduce the third term to penalize every station visit, which is plausible because we only visit a charging station when necessary under the EVRPTW setting. In addition, we penalize the negative battery level in the fourth term. All the other problem constraints are taken into account in the masking scheme introduced in Section V.

$$r(Y^{t_m}) = - \sum_{t=1}^{t_m} \omega(y^{t-1}, y^t) + \beta_1 \max\{-ev^{t_m}, 0\} \\ + \beta_2 S(Y^{t_m}) + \beta_3 \sum_{t=0}^{t_m} \max\{-b^t, 0\} \quad (5)$$

where  $\omega(y^{t-1}, y^t)$  is the weight on edge  $(y^{t-1}, y^t)$ ,  $S(Y^{t_m})$  is the number of station visit(s) along trajectory  $Y^{t_m}$ ,  $\beta_1$ ,  $\beta_2$  and  $\beta_3$  are three negative constants.

In the next section, we describe the methodology in details and explain how it applies to EVRPTW.

## V. METHODOLOGY

### A. The Attention Model

We propose an attention model to parameterize the "probability estimator",  $P(y^{t+1}|X^t, G^t, Y^t)$ , introduced in the previous section. The model consists of 3 components: an embedding component to represent the system state in a high-dimensional vector form; an attention component to estimate the probability for each vertex; and an LSTM decoder to restore the travel history. The key difference between the proposed model and the model presented in [14] is that we incorporate a graph embedding component to synthesize the local and global information of the graph. The model structure is illustrated in Figure 2.

1) *Graph Embedding*: We first map the model inputs  $X^t$  and  $G^t$  into a high dimensional vector space. The embedded model inputs are denoted as  $\hat{X}^t$  and  $\hat{G}^t$  respectively. More specifically, for vertex  $i$ , its local information array  $X_i^t = (x_i, z_i, e_i, l_i, d_i^t)$  is embedded to a  $\xi$  dimensional vector  $\hat{X}_i^t$  with a 1-dimensional convolutional layer. The embedding layer is shared among vertices. In addition, we have another 1-dimensional convolutional layer for global variables  $(\tau^t, b^t, ev^t)$ , mapping them to a  $\xi$ -dimensional vector  $\hat{G}^t$ .

We then utilize the Structure2Vec tool introduced in [16] to synthesize the embedded vectors. In particular, we initialize a vector  $\mu_i^{(0)} = \hat{X}_i^t$  for each vertex  $i$ , and then update  $\mu_i^{(k)}, \forall k = 1, 2, \dots, p$  recursively using Equation (6). After  $p$  rounds of recursion, the network will generate a  $\xi$ -dimensional vector  $\mu_i^{(p)}$  for each vertex  $i$  and we set  $\mu_i^t$  to  $\mu_i^{(p)}$ .

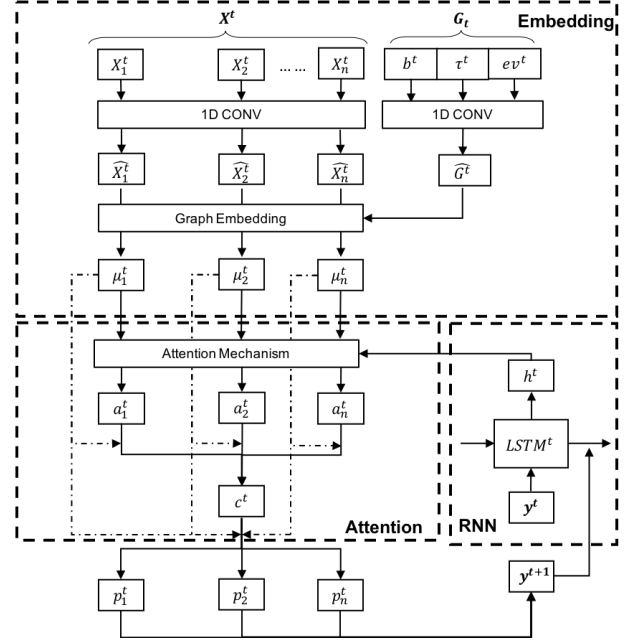


Fig. 2. The proposed attention model.

$$\mu_i^{(k)} = \text{relu}\{\theta_1 \hat{X}_i^t + \theta_2 \hat{G}^t + \theta_3 \sum_{j \in N(i)} \mu_j^{(k-1)} + \theta_4 \sum_{j \in N(i)} \text{relu}[\theta_5 w(i, j)]\} \quad (6)$$

where  $N(i)$  is the neighborhood of the vertex  $i$ ,  $w(i, j)$  represents the weight on edge  $(i, j)$ ,  $\theta_1$ ,  $\theta_2$ ,  $\theta_3$  and  $\theta_4$  are trainable variables.

At each round of recursion, the global information and location information are aggregated by the first two terms of Equation (6), while the information at different vertices and edges propagates among each other via the last two summation terms. The final embedded vectors  $\mu_i^t$  contains both local and global information, thus could better represent the complicated context of the graph.

2) *Attention Mechanism*: Based on the embedded vectors  $\mu_i^t$ , we utilize the context-based attention mechanism proposed by [22] to calculate the visiting probability of each vertex  $i$ .

We first calculate a context vector  $c^t$  specifying the state of the whole graph as a weighted sum of all embedded vectors, as shown in Equation (7). The weight of each vertex is defined in Equations (8) and (9).

$$c^t = \sum_{i=0}^{M+N} a_i^t \mu_i^t, \quad (7)$$

$$a_i^t = \text{softmax}(v_i^t) \quad (8)$$

$$v_i^t = W_v \tanh\{W_u [\mu_i^t; h^t]\} \quad (9)$$

where  $v_i^t$  is the  $i^{th}$  entry of vector  $v^t$ ,  $h^t$  is the hidden state of the LSTM decoder,  $W_v$  and  $W_u$  are trainable variables.  $[:]$  means concatenating the two vectors on the two sides of the symbol ":",

Then, we estimate the probability of visiting each vertex  $i$  at the next, step  $p_i^t$ , as in Equations (10) and (11).

$$p_i^t = \text{softmax}(g^t) \quad (10)$$

$$g_i^t = W_g \tanh(W_c[\mu_i^t; c_t]). \quad (11)$$

where  $g_i^t$  is the  $i^{th}$  entry of vector  $g^t$ ,  $W_c$  and  $W_g$  are trainable variables.

3) *Masking Scheme*: In order to accelerate the training process and ensure solution feasibility, we design several masking schemes to exclude infeasible routes. In particular, suppose that the EV is currently at vertex  $i$  at decoding step  $t$ , if vertex  $j$ ,  $\forall j \neq i$  satisfies one of the following conditions, we assign a very large negative number to the corresponding  $v_j^t$  and  $g_j^t$  such that the calculated weight  $a_j^t$  and probability  $p_j^t$  will be very close, if not equal, to 0:

- Vertex  $j$  represents a customer, its unsatisfied demand is zero or exceeds the remaining cargo of the EV;
- Vertex  $j$  represents a customer, the EV's current battery level  $b^t$  can not support the EV to complete the trip from vertex  $i$  to vertex  $j$  and then to the depot;
- The earliest arrival time at vertex  $j$  still violates its time window constraint;
- Given  $\tau^t$ , the travelling time from vertex  $i$  to  $j$  and the recharging time at vertex  $j$ , if vertex  $j$  is a station, will result in violations of the planning horizon constraint;
- We mask all the vertices except the depot if the EV is currently at the depot and there is no remaining cargo at any customer vertices.

4) *LSTM Decoder*: Similar to [14], we use the LSTM to model the decoder network. At decoding step  $t$ , The LSTM intakes the vector representation of the EV's current position  $\hat{X}_{y^t}^t$  as well as the hidden state from the previous decoding step  $h^{t-1}$  and output a hidden state  $h^t$  maintaining information about the trajectory up to step  $t$ , i.e.  $Y^t$ . The hidden state  $h^t$  is then fed to the attention model as introduced earlier in this section.

## B. Decoding Methods

At each decoding step  $t$ , we determine the next vertex to visit according to the estimated probability  $p_i^t, \forall i$ . In particular we consider three decoding methods:

- **Greedy Decoding**: greedily select the vertex with the highest probability at each decoding step;
- **Stochastic Sampling**: Sample the trajectory based on the estimated probability distribution;
- **Beam Search**: maintain multiple trajectories simultaneously, and finally select the trajectory with the highest overall probability.

In order to let the model see as many different conditions as possible during training, we use the stochastic sampling to train the model. All the three decoding methods are implemented and compared when testing.

## C. Policy Gradient

We implement a policy gradient algorithm to train the model. The basic idea is that, instead of letting the model learn from optimal solutions provided by existing algorithms, we use the reward function defined earlier to evaluate the quality of the solutions generated by the model. In each training iteration, we use  $\theta$  to demote all the trainable variables in the current mode, and  $\pi^\theta$  to denote the corresponding stochastic solution policy. we use  $\pi^\theta$  to sample solutions for a batch of  $N$  randomly generated instances, and calculate the corresponding rewards. Based on the rewards, we estimate the gradient of a loss function with respect to each trainable variable. We then use the Adam optimizer [23] to update the trainable variables in the model.

When estimating gradients, a good baseline usually reduce training variance and therefore increase speed of learning [15]. Instead of using the A3C methods as in [14] which is difficult to implement in practice, we employ the rollout baseline as proposed by [15]. More specifically, in the first  $\Lambda$  training steps, we simply use the exponential moving average of the rewards obtained by the model. At the  $\Lambda^{th}$  step, we set the baseline policy to the policy we have at the end of the  $\Lambda^{th}$  step. After that, we evaluate the baseline policy every  $\zeta$  iterations. We update the baseline policy if and only if the current policy is significantly better than the baseline policy on a separate test set according to a paired t-test ( $\alpha = 5\%$ ). We generate a new test set every time the baseline policy is updated.

In particular, we define the key components of the policy gradient method as follows:

1) *Loss Function*: We aim to minimize the loss function as shown in Equation (12). The loss function represents the negative expected total reward of the trajectory  $Y$  sampled using the stochastic policy  $\pi^\theta$ .

$$L(\theta) = -E_{Y \sim \pi^\theta} [r(Y)] \quad (12)$$

2) *Gradient Estimation*: We use Equation (13) to estimate the gradient of the loss function  $L(\theta)$  with respect to the trainable variables  $\theta$ . The parameter  $N$  is the batch size,  $X_{[i]}$  is the  $i^{th}$  training example in the batch, and  $Y_{[i]}$  is the corresponding solution generated using  $\pi^\theta$ . Additionally,  $BL()$  represents the rollout baseline introduced in [15], and  $P_\theta(Y_{[i]}|X_{[i]})$  indicates the probability of generating solution  $Y_{[i]}$  given training example  $X_{[i]}$  using stochastic policy  $\pi^\theta$ . We use the probability chain rule put forward by [19] to decompose the probability  $P_\theta(Y_{[i]}|X_{[i]})$  as in Equation (14). Terms  $P_\theta(y_{[i]}^{t+1}|X_{[i]}^t, G_{[i]}^t, Y_{[i]}^t)$  on the right hand side could be obtained from the model at each decoding step.

$$\nabla_\theta L = \frac{1}{N} \sum_{i=1}^N [r(Y_{[i]}) - BL(X_{[i]})] \nabla_\theta \log P_\theta(Y_{[i]}|X_{[i]}) \quad (13)$$

where

$$P_\theta(Y_{[i]}|X_{[i]}) = \prod_{t=0}^{|Y_{[i]}|-1} P_\theta(y_{[i]}^{t+1}|X_{[i]}^t, G_{[i]}^t, Y_{[i]}^t) \quad (14)$$

3) *Instance Generation*: At each training step, we generate  $N$  random EVRPTW training instances. In each instance, the vertices are uniformly distributed among a region  $[0, 1] \times [0, 1]$ . Customer demands are considered discrete, they are randomly selected from  $\{0.05, 0.10, 0.15, 0.20\}$  with equal probabilities. We use a way similar to [24] to generate the time window for each customer. The center of a time window is uniformly distributed among  $[0, 1]$  while the length is normally distributed with mean 0.2 and standard deviation 0.05. The time windows are trimmed, if necessary, to fit the planning horizon  $[0, 1]$ . We note that although the feasibility of the instances generated by this method is not guaranteed, according to our experiment, they are actually feasible in most cases. Since deep learning model in general is robust to random errors in training data, we do not apply any adjustments to those infeasible instances.

We normalize the vehicle specifications in [3] to the interval  $[0, 1]$ . Cargo and battery capacities of each EV are set to 1.0. Fully charging an EV from 0 requires time 0.25. Charging the energy consumed when travelling one unit of distance requires time 0.15. The planning horizon is  $[0, 1.0]$ . We consider a fleet of 3 EVs serving 10 customers in a region with 3 stations during training. We use this small instance size to enhance the instance generation efficiency. According to our numerical experiments, this does not compromise the model performance. Test data are generated in the same way as we produce training data, yet the numbers of customers, stations and EVs could vary.

The pseudo code of the training procedure is summarized in Algorithm 1.

## VI. NUMERICAL EXPERIMENT

### A. Experimental Setting

We perform all the tests using a Macbook Pro (2018) running Mac OS 10.13.6 with 4 CPU processors at 2.3 GHZ and 16 GB of RAM. The RL model is realized using Tensorflow 2.2.0. The code is implemented in Python.

For the RL model, we adapt most hyper-parameters from the work done by [14]. We use two separate 1-dimensional convolutional layers for the embeddings of local and global information respectively. All this information is embedded in a 128-dimensional vector space. We utilize an LSTM network with a state size of 128. For the Adam optimizer [23], we set the initial step size to 0.001, and the batch size to  $N = 128$ . To stabilize the training, we clip the gradients such that their norms are no more than 2.0. With regard to the rollout baseline, we use the moving exponential average baseline in the first 1000 training steps and evaluate the baseline policy every 100 training steps after that. In the reward function, the penalty factors for depot and station visits as well as negative battery level are set to 1.0, 0.3 and 100 respectively. All the trainable variables are initialized with the Xavier initialization [25]. We train the model for 10000 iterations which takes approximately 90 hours.

When training the model, we sample the solutions in a stochastic manner to diversify the possible circumstances encountered by the model. When testing, we consider all the three decoding methods and compare their performance. We

---

### Algorithm 1: REINFORCE with Rollout Baseline

---

```

initialize the network weights  $\theta$ , and test set  $S$ ;
for  $i = 1, 2, \dots$  do
    generate  $N$  random instances  $X_{[1]}, X_{[2]}, \dots, X_{[N]}$ ;
    for  $n = 1, 2, \dots, N$  do
        initialize step counter  $t_n \leftarrow 0$ ;
        repeat
            choose  $y_{[n]}^{t_n+1}$  according to the probability
            distribution  $P_\theta(y_{[n]}^{t_n+1} | X_{[n]}^{t_n}, G_{[n]}^{t_n}, Y_{[n]}^{t_n})$ ;
            observe new state  $X_{[n]}^{t_n+1}, G_{[n]}^{t_n+1}, Y_{[n]}^{t_n+1}$ ;
             $t_n \leftarrow t_n + 1$ ;
        until termination condition is satisfied;
        compute reward  $r(Y_{[n]}^{t_n})$ ;
    end
    if  $i \leq \Lambda$  then
         $BL(X_{[i]}) \leftarrow \text{avg} [r(Y_{[1]}^{t_1}), \dots, r(Y_{[N]}^{t_N})]$ ;
    else
         $BL(X_{[i]}) \leftarrow \pi^{BL}(X_{[i]})$ ;
    end
     $d\theta = \frac{1}{N} \sum_{i=1}^N [r(Y_{[i]}) - BL(X_{[i]})] \nabla_\theta \log P_\theta(Y_{[i]} | X_{[i]})$ ;
     $\theta \leftarrow \text{Adam}(\theta, d\theta)$ ;
    if  $i = \Lambda$  then
        initialize baseline  $\pi^{BL} \leftarrow \pi^\theta$ ;
    else
        if  $i \bmod \zeta = 0$  and
         $\text{OneSideTTest}(\pi^\theta(S), \pi^{BL}(S)) < \alpha$  then
             $\pi^{BL} \leftarrow \pi^\theta$ ;
            create new test set  $S$ ;
        end
    end
end

```

---

note that when implementing stochastic decoding for test, we sample 100 solutions for each instance and report the solution with the shortest total distance. For beam search, we maintain 3 solutions simultaneously and report the one with the highest overall probability.

### B. Computational Result

We compare the performance of three methodologies: CPLEX, the VNS/TS heuristic developed by Schneider et al. [3], and the reinforcement learning model we proposed in Tables I and II.

We apply these solution approaches to six different scenarios whose names indicate the numbers of customers, stations, and available EVs. For example, "C5-S2-EV2" means the scenario of 5 customers, 2 charging stations and 2 EVs. For each scenario, we solve 100 instances created in the same way as we produce the training data and report the mean total distance travelled by the EV fleet and the gap with respect to the minimal distance achieved by these algorithms in Table I. The average solution time in seconds over the 100 instances in seconds is recorded in Table II. We only report the results

TABLE I  
COMPARISON OF AVERAGE TOTAL TRAVEL DISTANCE OF THE 5 APPROACHES

Instance	CPLEX		VNS/TS		RL(Stochastic)		RL(Greedy)		RL(Beam)	
	Distance	Gap	Distance	Gap	Distance	Gap	Distance	Gap	Distance	Gap
C5-S2-EV2	<b>2.33</b>	0.00%	2.33	0.40%	2.53	8.58%	2.67	14.59%	2.64	13.30%
C10-S3-EV3	<b>3.64</b>	0.00%	3.64	0.85%	4.07	11.81%	4.39	20.60%	4.38	20.33%
C20-S3-EV3	-	-	<b>5.34</b>	0.00%	6.41	20.04%	7.27	36.14%	7.48	40.07%
C30-S4-EV4	-	-	<b>6.87</b>	0.00%	8.46	23.14%	9.76	42.07%	10.58	54.00%
C40-S5-EV5	-	-	-	-	<b>11.17</b>	0.00%	12.70	13.70%	14.72	31.78%
C50-S6-EV6	-	-	-	-	<b>14.32</b>	0.00%	16.46	14.94%	18.64	30.17%
C100-S12-EV12	-	-	-	-	<b>41.53</b>	0.00%	43.01	3.56%	58.85	41.70%

TABLE II  
COMPARISONS OF AVERAGE SOLUTION TIME OF THE 5 APPROACHES

Instance	CPLEX	VNS/TS	RL(stochastic)	RL(Greedy)	RL(Beam)
C5-S2-EV2	0.03	1.32	2.88	0.17	0.20
C10-S3-EV3	67.65	10.37	7.63	0.35	0.40
C20-S3-EV3	-	168.86	19.40	0.62	0.71
C30-S4-EV4	-	536.80	43.06	1.06	1.17
C40-S5-EV5	-	-	70.26	1.69	1.86
C50-S6-EV6	-	-	107.96	2.31	2.61
C100-S12-EV12	-	-	401.30	7.89	8.87

for algorithms that can successfully solve an instance within 15 minutes.

As shown, although more time-consuming than the greedy decoding and beam search, the stochastic decoding approach always yields solutions with the best quality among the three reinforcement learning implementations. This finding is consistent with the results presented in [12] that learning a policy which directly produces a single, optimal solution is often impractical. Instead, exploring the solution space with the stochastic policy usually lead to solutions better than a single "best-guess". However, even the performance of the stochastic decoding is far from the state of the art. For scenarios "C5-S2-EV2" and "C10-S3-EV3", the optimality gaps are 8.58% and 11.81% respectively, which are worse than CPLEX and the VNS/TS heuristic.

The proposed model showcases better scalability and generalization capability than CPLEX and the VNS/TS heuristic. When it comes to the scenarios with 20 or more customers, similar to the results reported in [3], CPLEX is not able to solve the problem within reasonable time. The VNS/TS heuristic outperforms the RL model in terms of solution quality on scenarios "C20-S3-EV3" and "C30-S4-EV4", yet spends 7-10 times the solution time utilized by the RL model. The gaps between the distances accomplished by the VNS/TS heuristic and the RL model are 20.04% and 23.14% respectively for these two scenarios. Regarding scenarios with 40 or more customers, the RL model is the only algorithm that is able to solve the EVRPTW within 15 minutes. In fact, the RL model only spends on average around 1.8 minutes to solve an instance with 50 customers.

### C. Algorithm Analysis

In this section, we perform detailed analysis on the proposed attention model by visualizing the routes generated by it and comparing them with the ones produced by the VNS/TS

heuristic. In Figure 3, we present the sample routes generated by the two algorithms. The sub-figures in each row are for the same instance. Within each row, the sub-figures on the left and in the middle are produced by the VNS/TS heuristic and the stochastic implementation of the RL model respectively. The sub-figure on the right shows the time windows of the vertices. Elements corresponding to customers, charging stations, and the depot are labelled in different colors.

One interesting observation from the first instance is that the RL model is able to make the routing decision based on the vertices' locations and time windows. The two EVs both start their route with a vertex (vertices 3 and 8) whose time window begins relatively early and then move to other vertices roughly following the start time of their time windows. However, there are some exceptions. Taking the route in black as an example, when leaving from vertex 6, instead of directly going to vertex 10 whose time window starts earlier, it first moves to vertex 2 such that the overall travelling distance is reduced. Similar rules apply when considering the order of vertices 6 and 8. Although the model fails to identify the optimal order of vertices 4 and 7 which makes the sole difference between the two route figures, the model showcases its capability of synthetically considering location and time information which is not very straightforward even for human beings.

It is also very interesting to visualize the attention mechanism for the proposed model. In Figure 4, we visualize the intermediate output  $a_i^t$  at different decoding steps of the same instance. The darker a vertex is, the greater attention it receives from the RL model. At the very beginning, the model puts attentions on various vertices with especial focuses on the vertices on the right (vertices 9, 4 and 7). After it takes the first move to vertex 8, most of its attentions are placed on vertices on the left (vertices 2, 6, 1, 10) which form the first route later on. And then, at step 7, the model's attentions, again, go to all the unsatisfied customers, charging stations as well as the

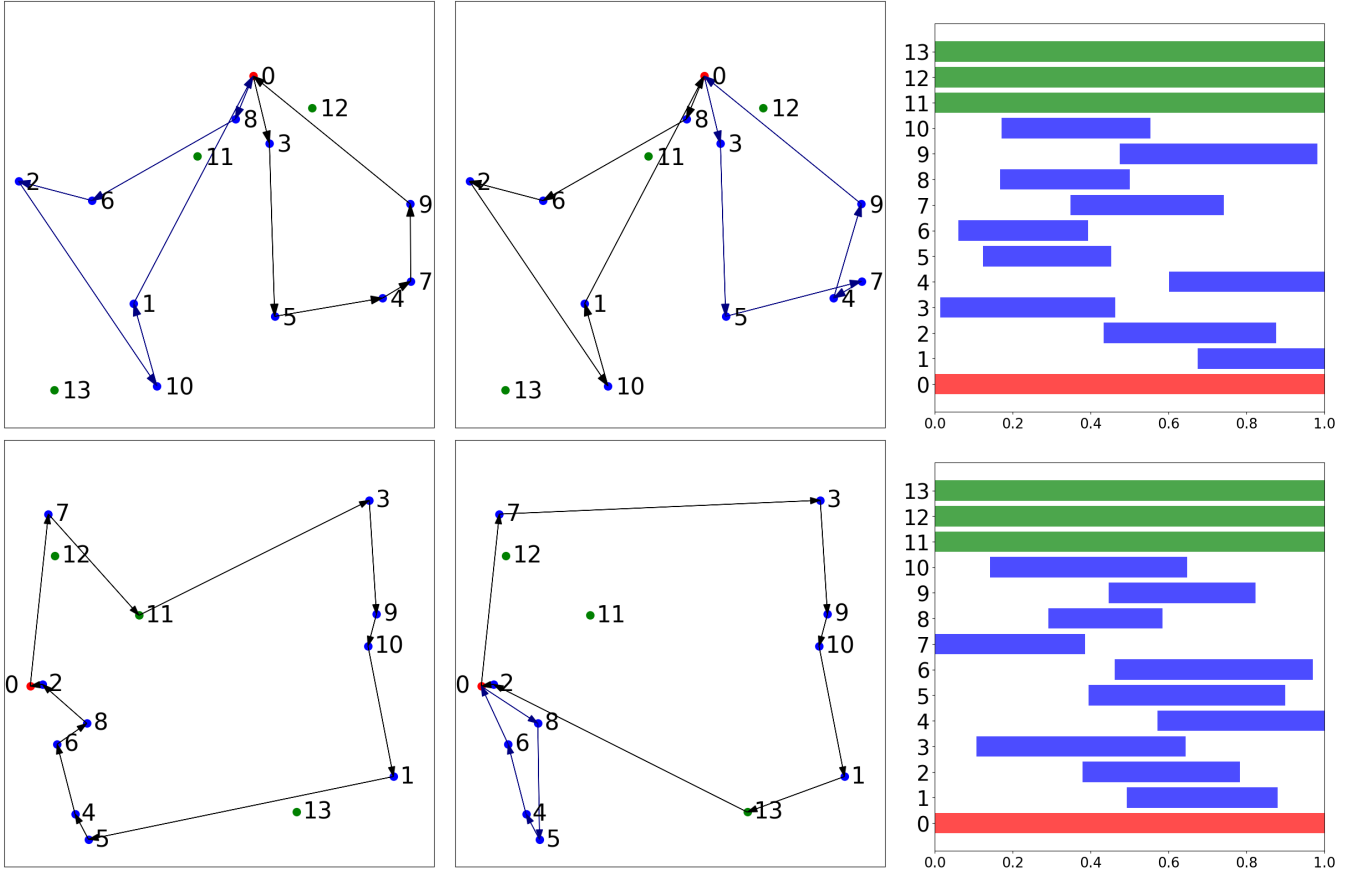


Fig. 3. Sample routes for 2 instances, each with 10 customers, 3 charging stations and 3 EVs, generated by the VNS/TS heuristic (on the left) and the stochastic implementation of the RL model (in the middle). The figure on the left visualizes the time windows of the vertices. Depot-, station- and customer-related vertices and bars are in red, green and blue respectively. Figures in the same row correspond to the same instance.

depot, and evolve as the EV travels. We note that, at step 9, the model appears to lose attention on any of the vertices. And it is right after this step (step 10) that the model makes a bad decision to visit vertex 7 before visiting vertex 4. Moreover, it is worth noting that, throughout the whole solution process, the depot (vertex 0) along with the charging stations (vertices 11, 12, and 13) on average receive greater attention comparing to customers. And the attentions on the station and depot increase as the EV travels along its route (from steps 1 to 6 and from steps 7 to 12). This could be explained by the fact that as EV travels along its route, its battery level becomes lower and lower, making it more and more important to consider visiting vertices where it can charge the battery.

Nevertheless, we also find that the RL model is sometimes short-sighted and is not able to identify some more complicated structures embedded in the graph. For the second instance in Figure 3, the VNS/TS heuristic utilizes only one EV to serve all the customers while the RL model needs two. The reason is that, in the route generated by the VNS/TS heuristic, the EV charges its battery early in its trip when the time windows are relatively loose so that it has enough energy and will not miss the time windows for the later vertices. One EV in the RL model's solution actually takes a very similar route, however, it doesn't take the detour to vertex 11 to charge. When the model finally realizes that the EV does not have enough energy to complete the trip, it lets the

EV to visit station 13 after vertex 1. This detour along with time spent at the charging station makes the EV miss the time window of vertex 8, thus results in the usage of the second EV.

In summary, the RL model is able to at least partially understand the given graph and generate relatively good routes accordingly. Even if the routes are obviously not optimal, the capability of quickly capturing the most basic but important information makes the RL model very attractive, especially in large-scale real-time implementations.

## VII. CONCLUSION

In this research, we develop a reinforcement learning framework for solving the EVRPTW. Although the solutions generated by the proposed algorithm are in general far from the state of the art, we believe it is very promising in practice. The reasons are two-fold. First, the algorithm showcases great scalability. It is able to solve instances of very large sizes which are unsolvable with any existing methods. Our analysis shows that the proposed model is able to quickly capture important information embedded in the graph, and then effectively provide relatively good feasible solutions to the problem. Though not optimal, those good feasible solutions could be utilized to support large-scale EV operations. Secondly, the proposed model is very efficient in solving the EVRPTW.



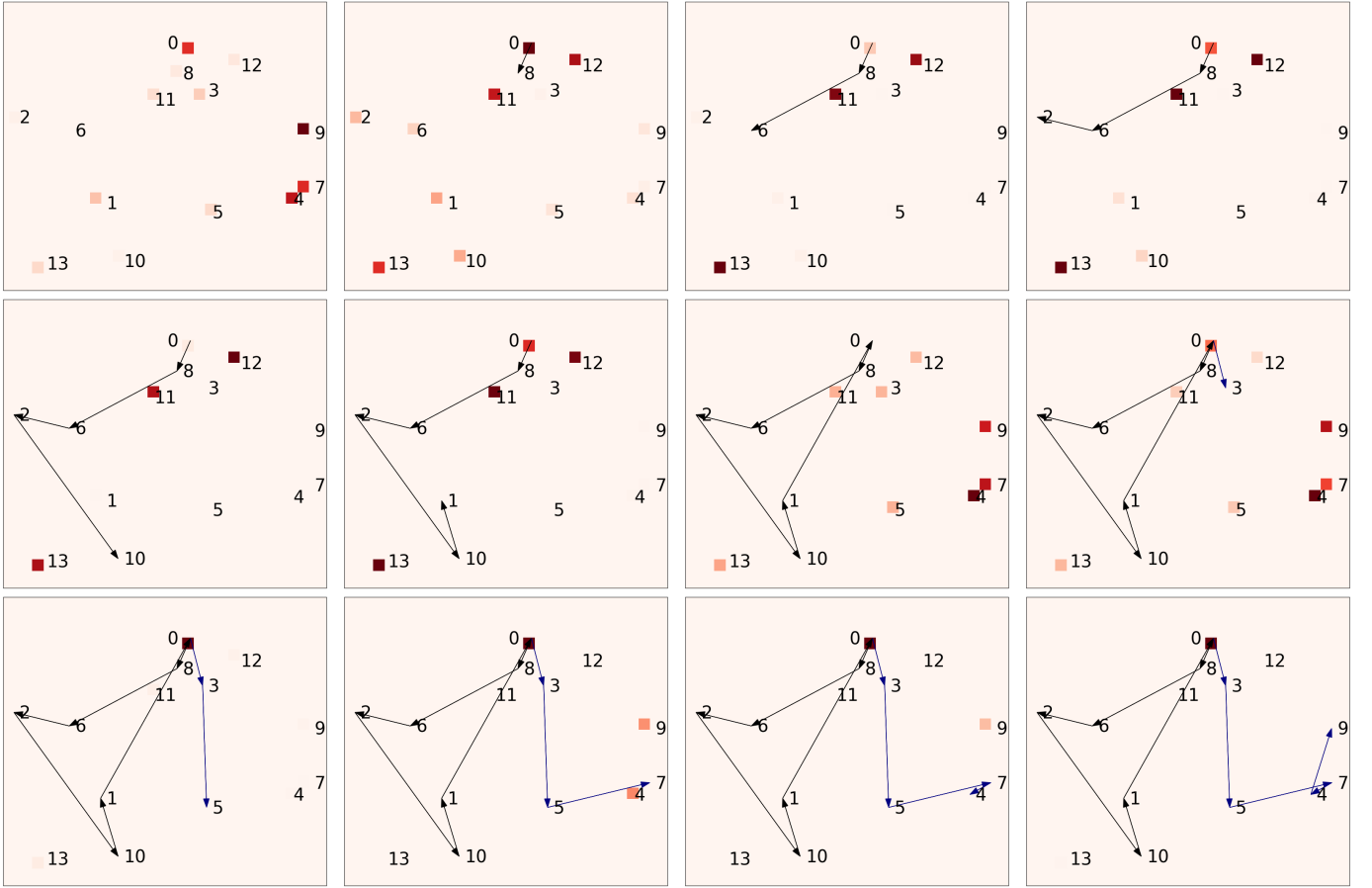


Fig. 4. Visualization of the attention mechanism on sample instance one. Each of the sub-figures (from left to right then top to bottom) shows the attention weights the RL model put on the vertices. The values of the weights are normalized such that it is easier to observe the relative importance of the vertices. The darker a vertex is, the higher weight it is assigned.

In practice, lots of components in the graph, such as customers' demands and time windows as well as the availability of charging services, could change instantaneously. The RL model's ability to efficiently solve the problem allows the EV operators to quickly make adjustments so as to tackle the challenges coming from the stochastic nature of the EVPTW. Thirdly, the proposed model has potential in generalizing to other variants of the EVRPTW. Practitioners can generalize the proposed method by slightly tailoring the masking schemes as well as the reward function according to their own operational constraints and objectives, which is much easier than adjusting other exact or meta-heuristic algorithms that usually requires extensive hand-engineering and domain knowledge.

From a theoretical point of view, the proposed solution approach incorporates the graph embedding techniques with the PN architecture, allowing the algorithm to synthesize the local and global information to solve the target problem. We believe its applications are not limited to solving EVRPTW. It could fit with other CO problems that consider both local and global states of the graph on which it is defined.

Finally, we highlight several potential extensions of the proposed approach. First, we could apply some local search heuristic to the solution generated by the model to further enhance solution quality. It is also possible to exploit the gen-

erated feasible solutions to support other solution approaches. For instance, we could use the feasible solutions to trim the search tree of traditional MIP solvers. The feasible solutions can also be used as the search starting points for other meta-heuristics such as the VNS/TS.

#### ACKNOWLEDGMENT

Bo Lin was supported by the Energy Council of Canada energy policy research fellowship and Bissan Ghaddar was supported by NSERC Discovery Grant 2017-04185.

#### REFERENCES

- [1] A. G. Boulanger, A. C. Chu, S. Maxx, and D. L. Waltz, "Vehicle electrification: Status and issues," *Proceedings of the IEEE*, vol. 99, no. 6, pp. 1116–1138, 2011.
- [2] R. A. Waraich, M. D. Galus, C. Dobler, M. Balmer, G. Andersson, and K. W. Axhausen, "Plug-in hybrid electric vehicles and smart grids: Investigations based on a microsimulation," *Transportation Research Part C: Emerging Technologies*, vol. 28, pp. 74–86, 2013.
- [3] M. Schneider, A. Stenger, and D. Goetz, "The electric vehicle-routing problem with time windows and recharging stations," *Transportation Science*, vol. 48, no. 4, pp. 500–520, 2014.
- [4] G. Desaulniers, F. Errico, S. Irnich, and M. Schneider, "Exact algorithms for electric vehicle-routing problems with time windows," *Operations Research*, vol. 64, no. 6, pp. 1388–1405, 2016.
- [5] O. Vinyals, M. Fortunato, and N. Jaitly, "Pointer networks," in *Advances in neural information processing systems*, 2015, pp. 2692–2700.

- [6] Z. Li, Q. Chen, and V. Koltun, “Combinatorial optimization with graph convolutional networks and guided tree search,” in *Advances in Neural Information Processing Systems*, 2018, pp. 539–548.
- [7] D. Selsam, M. Lamm, B. Bünz, P. Liang, L. de Moura, and D. L. Dill, “Learning a SAT solver from single-bit supervision,” in *International Conference on Learning Representations*, 2019.
- [8] M. Prates, P. H. Avelar, H. Lemos, L. C. Lamb, and M. Y. Vardi, “Learning to solve np-complete problems: A graph neural network for decision tsp,” in *Proceedings of the AAAI Conference on Artificial Intelligence*, vol. 33, 2019, pp. 4731–4738.
- [9] I. Bello, H. Pham, Q. V. Le, M. Norouzi, and S. Bengio, “Neural combinatorial optimization with reinforcement learning,” in *International Conference on Learning Representations Workshop*, 2017.
- [10] W. Zhang and T. G. Dietterich, “A reinforcement learning approach to job-shop scheduling,” in *IJCAI*, vol. 95. Citeseer, 1995, pp. 1114–1120.
- [11] S. Manchanda, A. Mittal, A. Dhawan, S. Medya, S. Ranu, and A. K. Singh, “Learning heuristics over large graphs via deep reinforcement learning,” *CoRR*, vol. abs/1903.03332, 2019. [Online]. Available: <http://arxiv.org/abs/1903.03332>
- [12] T. D. Barrett, W. R. Clements, J. N. Foerster, and A. I. Lvovsky, “Exploratory combinatorial optimization with reinforcement learning,” in *Proceedings of the AAAI conference*, 2020, pp. 3243–3250.
- [13] E. Khalil, H. Dai, Y. Zhang, B. Dilikina, and L. Song, “Learning combinatorial optimization algorithms over graphs,” in *Advances in Neural Information Processing Systems*, 2017, pp. 6348–6358.
- [14] M. Nazari, A. Oroojlooy, L. Snyder, and M. Takác, “Reinforcement learning for solving the vehicle routing problem,” in *Advances in Neural Information Processing Systems*, 2018, pp. 9839–9849.
- [15] W. Kool, H. van Hoof, and M. Welling, “Attention, learn to solve routing problems!” in *7th International Conference on Learning Representations, ICLR*, 2019. [Online]. Available: <https://openreview.net/forum?id=ByxBFsRqYm>
- [16] H. Dai, B. Dai, and L. Song, “Discriminative embeddings of latent variable models for structured data,” in *International conference on machine learning*, 2016, pp. 2702–2711.
- [17] J. J. Hopfield and D. W. Tank, ““neural” computation of decisions in optimization problems,” *Biological cybernetics*, vol. 52, no. 3, pp. 141–152, 1985.
- [18] G. Wilson and G. Pawley, “On the stability of the travelling salesman problem algorithm of hopfield and tank,” *Biological Cybernetics*, vol. 58, no. 1, pp. 63–70, 1988.
- [19] I. Sutskever, O. Vinyals, and Q. V. Le, “Sequence to sequence learning with neural networks,” in *Advances in neural information processing systems*, 2014, pp. 3104–3112.
- [20] J. James, W. Yu, and J. Gu, “Online vehicle routing with neural combinatorial optimization and deep reinforcement learning,” *IEEE Transactions on Intelligent Transportation Systems*, vol. 20, no. 10, pp. 3806–3817, 2019.
- [21] J. Zhao, M. Mao, X. Zhao, and J. Zou, “A hybrid of deep reinforcement learning and local search for the vehicle routing problems,” *IEEE Transactions on Intelligent Transportation Systems*, 2020.
- [22] D. Bahdanau, K. Cho, and Y. Bengio, “Neural machine translation by jointly learning to align and translate,” in *International Conference on Learning Representations*, 2015.
- [23] D. P. Kingma and J. Ba, “Adam: A method for stochastic optimization,” in *3rd International Conference on Learning Representations, ICLR 2015*, Y. Bengio and Y. LeCun, Eds., 2015. [Online]. Available: <http://arxiv.org/abs/1412.6980>
- [24] M. M. Solomon, “Algorithms for the vehicle routing and scheduling problems with time window constraints,” *Operations research*, vol. 35, no. 2, pp. 254–265, 1987.
- [25] X. Glorot and Y. Bengio, “Understanding the difficulty of training deep feedforward neural networks,” in *Proceedings of the thirteenth international conference on artificial intelligence and statistics*, 2010, pp. 249–256.